



A New Approach for Quantitative Definition of Asymmetrical Loading Tunnels

Wei Liu¹ · Shuning Dong² · Shangxian Yin³ · Zhenxue Dai¹ · Bin Xu³ · Mohamad Reza Soltanian⁴ · Qingyang Yu¹

Received: 1 September 2021 / Accepted: 23 August 2022 / Published online: 9 September 2022
© The Author(s), under exclusive licence to Shiraz University 2022

Abstract

Asymmetric loads often occur at tunnel entrances or exits during shallow buried tunnel construction. Due to asymmetrical loads, structures are subjected to complex forces, and the design process of these tunnels is different from that of regular tunnels. Therefore, it is necessary to discriminate asymmetric tunnels quantitatively. Currently, determining whether a tunnel is subject to asymmetrical loads is based on the empirical maximum burial depths and surface slope angles listed in the Chinese Code for the Design of Railway Tunnel. However, in real geological conditions, the maximum burial depths and surface slope angles of the tunnel are not necessarily completely consistent with the Chinese Code; in other words, the continuous discrimination of asymmetric tunnels is not realized. In this paper, the surrounding rock stress ratio of the arch shoulder was treated as index to define asymmetrical loading tunnels and a new approach to achieve the continuous discrimination of asymmetric tunnels was proposed. Compared to the empirical values in the Chinese Code, the results show that the asymmetric stress ratio tends to decrease with the decrease in the surrounding rock grade. Regardless of whether the grade is III, IV_{Rock}, IV_{Soil} or V, the asymmetric stress ratios of the surrounding rock tend to converge and stabilize with increasing burial depths and decreasing dip angles, and the sensitivity of the slope angle to the stress ratio is bounded by 20°. The asymmetric stress ratio of the surrounding rock arch shoulder can be used as an index to ascertain whether a tunnel is subjected to asymmetric loads. When the surrounding rock grades are III and IV_{Rock}, the values calculated by the proposed approach are lower than the empirical values, and the approach is more conservative than the empirical method. When the surrounding rock grades are IV_{Soil} and V, the values calculated by the proposed approach are in good agreement with the empirical values. The approach of continuous discrimination of asymmetric tunnels proposed in this paper is reliable. The findings of this study can help for better understanding of the identification of asymmetrical loading tunnels, the design of support structures and the safety risk assessment of tunnels.

Keywords Asymmetrical loading tunnel · Finite element model · Quantitative definition · Stress ratio

1 Introduction

In tunnel engineering, asymmetric phenomena are common. Especially at the entrance and exit of a tunnel, asymmetrical loads are particularly prevalent (Yang et al. 2020; Hu et al. 2021; Liu et al. 2017). In contrast to symmetric tunnels, asymmetric tunnels are more complex in tunnel design and support structures (Xiao et al. 2014, 2016; Papanikolaou and Kappos 2014). Some scholars have studied the surrounding rock stress and the failure mechanism of asymmetrical loading tunnels, and many achievements have been obtained (Lei et al. 2015a, b; Lu et al. 2021; Zhao et al. 2021; Zhang et al. 2014; Qiu et al. 2021).

The first aspect is about the study of surrounding rock pressure calculation. Based on the calculation method of

✉ Qingyang Yu
qingyang@jlu.edu.cn

¹ College of Construction Engineering, Jilin University, Changchun, China

² Coal Technology & Engineering Group Corp, Xi'an Research Institute of China, Xi'an, China

³ Hebei State Key Laboratory of Mine Disaster Prevention, North China Institute of Science and Technology, Yanjiao, China

⁴ Department of Geology, University of Cincinnati, Cincinnati, USA

the code, modified computational equations of vertical load and horizontal load were proposed, and a simplified analytical method for surrounding rock pressure was given based on the new assumption condition and load simplified model (Zuo et al. 2011; Zhang et al. 2016). According to the bipolar coordinate system, Zou et al. (2018) proposed the Mohr–Coulomb failure criterion, the gravitational effect and elastic–plastic solutions for the rock surrounding a shallow tunnel in an elastic–plastic semi-infinite space. Using the complex variable method and discrete Fourier transform, Lin et al. (2019) presented a solution for the sectional estimation of the stress and displacement fields of a liner and a geomaterial near a shallow buried tunnel. In addition, Nomikos et al. (2006) presented an analytical method to calculate the load-carrying capacity of two-dimensional asymmetric rock wedges when the load on joint faces was not symmetric, such as the case of an asymmetric wedge formed in the roof of a circular tunnel in an inclined stress field. Furthermore, under the action of asymmetric loads, some scholars have proposed upper limit solutions of surrounding rock pressure, elastic solutions of plane strain and analytical solutions for the interaction of shallow buried tunnels (Lei et al. 2015a, b; Cao et al. 2019; Yang et al. 2013). By considering the mutation theory, strain hardening and softening and gravity of the cavity, some researchers have proposed the mutation model, rheological constitutive model and analytical model (Yang et al. 2019; Zuo et al. 2015).

The second aspect is about the study of failure mechanism and failure characteristics. Many scholars have obtained the stress distributions and variation trends of the surrounding rock by mechanical tests and numerical simulations (Li et al. 2020; Liu et al. 2017). Using numerical code realistic failure process analysis (RFPA), Wang et al. (2012) studied the failure mechanism for a circular tunnel in transversely isotropic rock. Based on field monitoring data, Xiao et al. (2014) conducted three-dimensional numerical modeling to simulate the process of tunnel construction and to analyze the mechanism of cracking in the secondary lining. The existence of an asymmetric load transforms the structural stress state, and the failure form differs depending on location. Using a tunnel excavation simulation testing system, the change laws and distribution forms of structural stress and surrounding rock pressure and the failure mechanism of the lining and surrounding rock in shallow buried tunnels under asymmetrical loading were studied systematically (Lei et al. 2016; Lei et al. 2015a, b). Based on similarity theory, a series of physical testing models and shaking table tests were designed and manufactured, and the dynamic response characteristics of shallow-buried tunnels with asymmetrical pressure distributions were obtained (Jiang et al. 2018a, b; Jiang et al. 2018a, b). Moreover, a unified displacement function is used as the displacement boundary condition of the cross section of each tunnel and can be used to capture

the asymmetric deformation behaviors about the horizontal and vertical centerlines (Kong et al. 2019). Based on the Lianchengshan tunnel, Chen et al. (2020) analyzed the change in rock mass pressure with deformation, time and distance from the excavation face by field monitoring and numerical simulation. Furthermore, with the DDA (discontinuous deformation analysis) method, Do et al. (2020) studied the mechanical response caused by horizontal excavation under different conditions (such as different inclinations and positions of the tunnel face). Using the direct boundary element method (BEM), Panji et al. (2016) studied the stress behavior of shallow buried tunnels under simultaneous non-uniform surface traction and asymmetric gravity loading, and the study showed that the shallow eccentricity of the load had a significant impact on the displacement and stress around the tunnel. By field observations, monitoring and three-dimensional (3D) numerical simulation, Yang et al. (2020) concluded that the retaining wall at the shallow side of a tunnel presents counterclockwise rotation deformation characteristics along the toe of the wall, and the covering soil at the wall surface can apply counterpressure to the retaining wall. Considering the most important parameters on overbreak, many ABC-ANN models have been constructed based on their effective parameters, and a new hybrid model, namely an artificial bee colony (ABC)–artificial neural network (ANN), has been developed to predict overbreak (Koo-pialipour et al. 2019).

The third aspect is about the study of stress ratio quantification, as shown in Table 1. By examining an example of a seismic cluster in a deep mine in Canada, a relative apparent stress ratio (ASR) was proposed to quantify the apparent stress of a seismic group, and the overall apparent stress of earthquakes was quantitatively calculated (Brown et al. 2017). To identify the deformation stage and failure process of a rock containing a single fissure, Lv et al. (2017) introduced the ratio of the concentrated stress to the peak stress of samples during experiments. In addition, Abdollahipour et al. (2012) defined the ratio of lateral stress to vertical stress as the stress ratio, and by the change in the ratio and the displacement of key points, the stability of the cavern was evaluated. Karatela et al. (2016) investigated the effect of fracture orientation and the in situ horizontal stress ratio on the stability of the rock mass around the borehole, and the results showed that when the in situ stress ratio increases, the rock blocks at the borehole wall tend to move toward the center of the borehole. Yu et al. (2020) defined the ratio of vertical stress as the stress ratio, and based on the Chinese Railway Tunnel Design Code, they quantitatively analyzed the stress ratio of two sides of asymmetrical loading tunnels. Furthermore, the influence of the dip angle and the ratio of horizontal and vertical stress on the bearing capacity of prestressed concrete-lined pressure tunnels was studied using a two-dimensional finite element model, and

Table 1 Summary of stress ratio

Name	Application	Principles	Advantages	Limitations
Relative apparent stress ratio (Brown et al. 2017)	Quantify the apparent stress of a seismic population	The ratio of the 80th percentile to the 20th percentile for a cumulative distribution of apparent stress	The ratio accounts for local variations in rock mass strength and mining depth and eliminates the requirement for arbitrary threshold values	Local experience is still needed to identify high apparent stress ratio conditions
Stress concentration strength ratio (Lv et al. 2017)	Divide deformation and failure process of fractured rock	The ratio of concentration stress to peak stress	The stages of deformation and failure process in rock loading are more accurately divided	The applicability under triaxial compression conditions needs to be further verified
Lateral stress to vertical stress ratio (Abdollahipour et al. 2012)	Assess cavern stability and sidewall displacement	The ratio of lateral stress to vertical stress	The predicted displacements are in good agreement with real values	The intermediate principal stress is neglected
In situ horizontal stress ratio (Kartala et al. 2016)	Assessment of the stability of rock mass around the borehole	The ratio of anisotropic stress	Introduced borehole stability criteria relevant to the extent of yielded zone and maximum displacement around the borehole	It is not possible to determine a definite threshold for the displacement of rock blocks for a particular condition
Asymmetric Stress Ratio (Yu et al. 2020)	Determine quantitative criteria for estimating the asymmetric stress	The ratio of vertical stress of tunnel arch shoulder	Provides a quantitative judgment for asymmetric tunnel	The process is cumbersome and dependent on the Chinese Code
In situ stress ratio (Simanjuntak et al. 2016)	Study on the bearing capacity of prestressed concrete-lined pressure tunnels	The ratio of horizontal stress to vertical stress	Identifying potential locations where longitudinal cracks may occur in the final lining	Applicability is limited
Empirical values of Chinese Code (TB 1003–2019)	Discriminate asymmetrical loading tunnel	Maximum burial depths and surface slope angles	Principle is simple	Subjectivity is strong and continuous discrimination cannot be achieved

the study revealed that the in situ stress ratio significantly affects the load sharing between the rock mass and the lining (Simanjuntak et al. 2016). In addition, studies have shown that when the tunnel diameter is fixed, the deeper the ground covering depth is, the greater the required limit support pressure. However, the ground covering depth has almost no effect on the ultimate support pressure, even if the tunnel is deep (Zhang et al. 2021). According to the Chinese Code for the Design of Railway Tunnels, determining whether a tunnel is subject to asymmetric loads is based on empirical values that are determined by maximum burial depths and surface slope angles (TB 1003–2019).

These studies have increased our understanding of the surrounding rock pressure calculation, failure mechanism, failure characteristics and quantification of stress ratio. However, very few studies have quantitatively analyzed the asymmetric loads of tunnels using the asymmetric stress ratio index. Furthermore, in the Chinese Code, asymmetrical loading tunnels are given by experience from the maximum burial depths and surface slope angles of the tunnel, and the continuous discrimination of asymmetric tunnels is not realized. In this study, numerical simulations were used to quantitatively analyze the stress ratio of the surrounding rock, and a new approach for achieving the

continuous discrimination of asymmetric tunnels was proposed. Compared to the Chinese Code, the new approach is relatively cumbersome. However, this method breaks through the constraints of a specific slope angle and buried depth, overcomes human subjective factors and realizes the continuous discrimination of asymmetrical loading tunnels. The methodology overview of this study is shown in Fig. 1. The results of this study provide significant insights for the identification of asymmetrical loading tunnels, design of support structures and safety risk assessment of tunnels.

2 Asymmetric Tunnel Stress Ratio Model

To eliminate the limitation and subjectivity of relying only on the empirical values listed in the Chinese Code (TB 1003–2019) to judge asymmetrical loading tunnels, finite element software was used to establish the 269 kinds of models with different burial depths and different ground slopes under different surrounding rock grades, and the asymmetric stress ratio of the arch shoulder under different conditions was quantitatively analyzed.

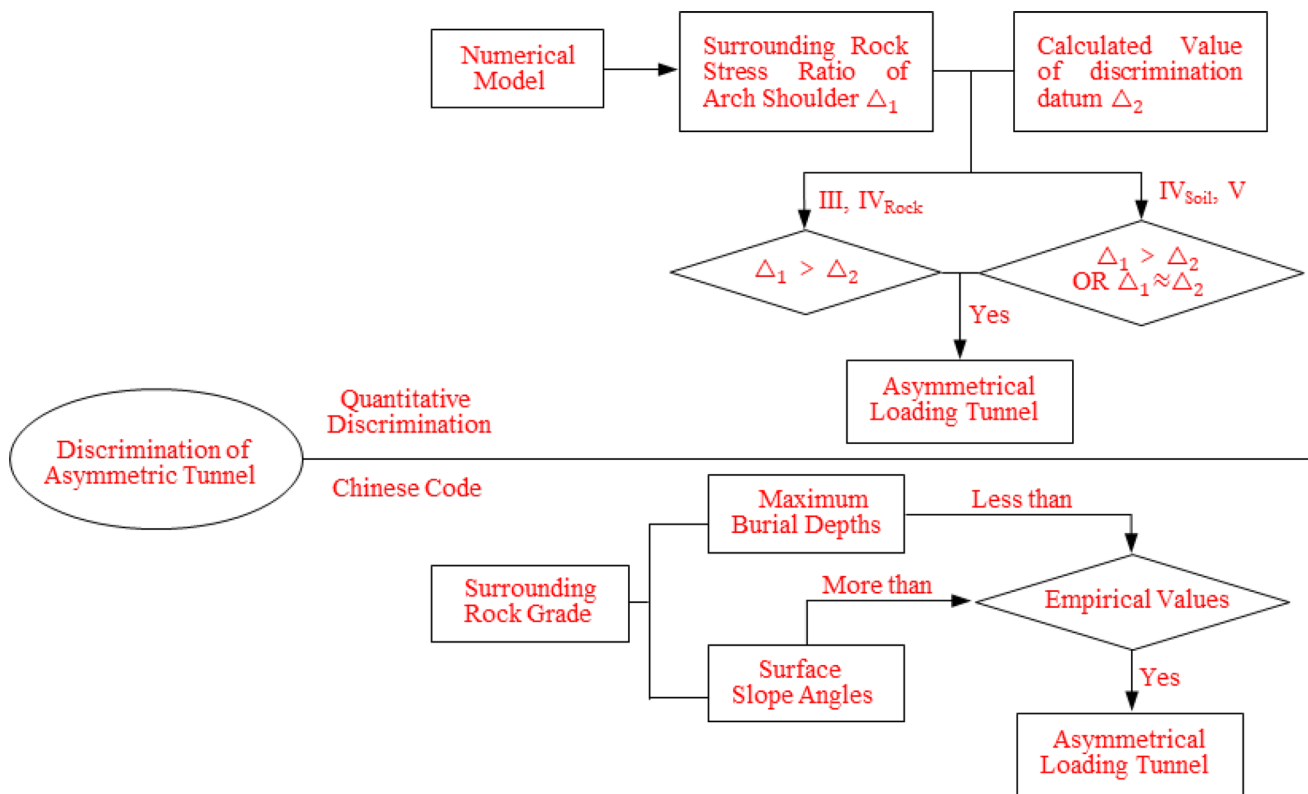


Fig. 1 Methodology overview

2.1 Elastic–plastic Mechanics Solution Model

In this study, the surrounding rock was considered to be an elastic–plastic material. When the stress state at a certain point in space enters the yield stage, the stress–strain relationship is nonlinear, and the increment of the total strain is made up of elastic strain and plastic strain on the basis of elastic–plastic theory (Wang et al. 2007):

$$d\{\varepsilon\} = d\{\varepsilon\}^e + d\{\varepsilon\}^p \quad (1)$$

The elastic–plastic constitutive relation of the surrounding rock is as follows:

$$\{d\sigma\} = \left[\begin{array}{c} [D_e] - \frac{[D_e] \left\{ \frac{\partial F}{\partial \sigma} \right\} \left\{ \frac{\partial F}{\partial \sigma} \right\}^T [D_e]}{\left\{ \frac{\partial F}{\partial \sigma} \right\}^T [D_e] \left\{ \frac{\partial F}{\partial \sigma} \right\} + A} \\ [D_e] \end{array} \right] d\{\varepsilon\} \quad (2)$$

Or abbreviated as:

$$\{d\sigma\} = ([D_e] - [D_p])d\{\varepsilon\} = [D_{ep}]d\{\varepsilon\} \quad (3)$$

where $[D_e]$ is the elastic matrix; $[D_p]$ is the plastic matrix; $[D_{ep}]$ is the elastic–plastic matrix; and $A = -\left\{ \frac{\partial F}{\partial \sigma} \right\} \{H\}$ is the characteristic parameter that can reflect the soft and hard characteristics of rock and soil materials, where $A=0$ corresponds to an ideal elastic–plastic material.

The expression of the elastic matrix $[D_e]$ of a material is as follows:

$$[D_e] = \begin{bmatrix} \lambda + 2G & \lambda & \lambda & 0 & 0 & 0 \\ \lambda & \lambda + 2G & \lambda & 0 & 0 & 0 \\ \lambda & \lambda & \lambda + 2G & 0 & 0 & 0 \\ 0 & 0 & 0 & G & 0 & 0 \\ 0 & 0 & 0 & 0 & G & 0 \\ 0 & 0 & 0 & 0 & 0 & G \end{bmatrix} \quad (4)$$

In contrast, the expression of the plastic matrix $[D_p]$ of a material is as follows:

$$[D_p] = \frac{[D_e] \left\{ \frac{\partial F}{\partial \sigma} \right\} \left\{ \frac{\partial F}{\partial \sigma} \right\}^T [D_e]}{\left\{ \frac{\partial F}{\partial \sigma} \right\}^T [D_e] \left\{ \frac{\partial F}{\partial \sigma} \right\} + A} \quad (5)$$

where λ is the lame constant and G is the shear modulus (kPa).

The plastic yield condition of rock and soil can be described according to the Mohr–Coulomb yield criterion as:

$$\tau_n = -\sigma_n \tan \varphi + c \quad (6)$$

With the yield function (f) of:

$$f = \frac{1}{2}(\sigma_1 - \sigma_3) + \frac{1}{2}(\sigma_1 + \sigma_3) \sin \varphi - c \cos \varphi \quad (7)$$

where τ_n is the shear stress (kPa), σ_n is the normal stress (kPa), φ is the internal friction angle, c is the cohesion coefficient (kN/m²), and σ_1 and σ_3 are the first and third principal stresses, respectively.

2.2 Boundary Conditions and Model Parameters

According to the geological conditions and the design parameters of the Shidaoyangcha tunnel, the span of the tunnel was taken to be 12.6 m and the height to be 10.0 m. Based on the principles of numerical model establishment, the width of the model in the X direction is 100 m, and the height of the model in the Z direction is 40 m from the bottom of the model to the center of the tunnel. The boundary is the displacement constraint. The two side boundaries are horizontal displacement constraints, the bottom boundary is x and y constraints, and the top boundary condition is an unconstrained boundary.

According to the support parameters of the Shidaoyangcha tunnel, the support structure is simulated by a linear elastic beam element and supported by C25 concrete with a thickness of 30 cm. The bolts are modeled as embedded truss elements with a length of 3.5 m and a spacing of 1.0 m. Depending on the characteristics of the surrounding rock, the initial geostress field considers only the overburden pressure of the surrounding rock, and other mechanical influences are ignored. The model assumes that the surrounding rock is an isotropic and homogeneous material. Tunnel excavation is simulated by the two-step method. A schematic of the calculation model is shown in Fig. 2a, and the finite element method (FEM) model is shown in Fig. 2b.

According to the Chinese Code for the Design of Highway Tunnels (JTG 3370.1–2018), the physical and mechanical parameters of the surrounding rocks are shown in Table 2.

2.3 Verifying the Model for Numerical Simulation

To verify the correctness of the numerical model, the stresses between the surrounding rock and initial lining of the shallow buried tunnel under asymmetric loads are monitored. Measuring points should be laid on the key points of representative sections, and the monitoring data of the arch shoulder were selected for analysis, as shown in Fig. 3a.

The compressive face of the pressure sensor should be oriented toward the surrounding rock, and the pressure sensor should be fixed on the steel arch frame before the initial lining is completed. Then, the shotcrete layer should be carefully

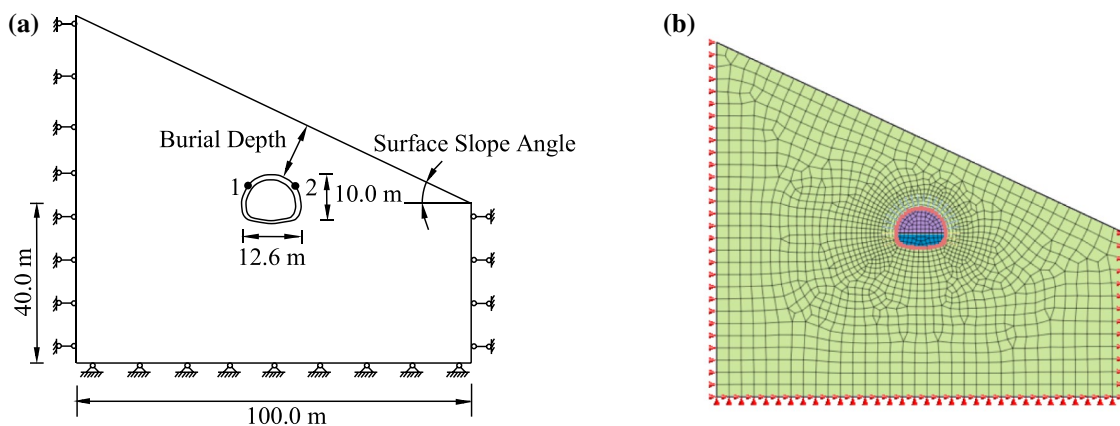
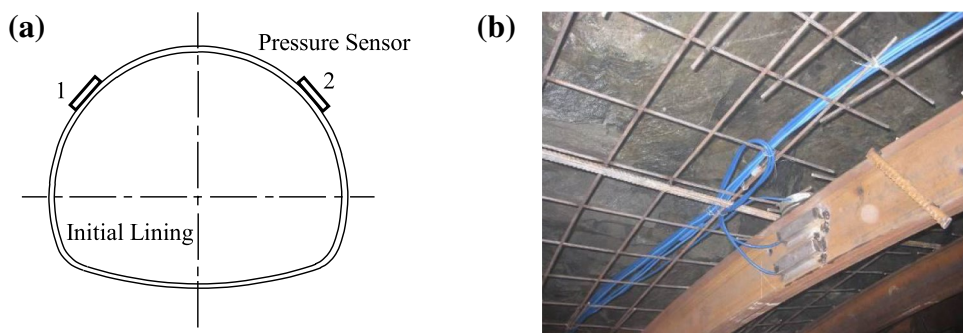


Fig. 2 Diagrams of the calculation model and FEM model for a tunnel under asymmetric loads: **a** geometric dimensional drawing of the tunnel model; **b** sectional drawing of the tunnel model

Table 2 Physical and mechanical parameters of surrounding rocks

Surrounding rock grade	Bulk density (kN/m ³)	Elastic modulus (GPa)	Poisson ratio	Internal friction angle (°)	Cohesion (kPa)
III	24	12	0.27	45	1100
IV Rock	23	5	0.30	38	600
IV Soil	20	2	0.35	30	300
V	18	1.5	0.40	25	100

Fig. 3 Layout of stress monitoring points of the tunnel: **a** position of pressure sensors; **b** arrangement of pressure sensors between the surrounding rock and initial lining



applied to prevent the formation of a gap between the shotcrete and the pressure sensor, as shown in Fig. 3b.

According to the numerical simulation, the corresponding simulated values of the asymmetric stress were obtained. A comparison of the stress monitoring results and the numerical simulation results is shown in Table 3. The results show that the numerical analysis agrees with the field measurements and that the numerical model is reliable.

Table 3 Comparison of the stress monitoring results and numerical simulation results

Serial number of the pressure sensor	Monitoring Sect. 1		Monitoring Sect. 2	
	1	2	1	2
Field measurement stress value (kPa)	192.12	285.74	298.60	339.81
FEM calculated stress value (kPa)	175.62	304.53	269.47	304.53

3 Stress Ratio and Numerical Models of Asymmetric Tunnels

3.1 Stress Ratio of Asymmetric Tunnels

At present, determining whether a tunnel is subject to asymmetric loads is based on the empirical values of the maximum burial depths and surface slope angles listed in the Chinese Code for the Design of Railway Tunnel (TB 1003–2019), which has great limitations and subjectivity. Therefore, to analyze the degree of asymmetric loads applied on the tunnel and realize the continuous discrimination of asymmetric tunnels, a quantitative approach to assess asymmetrical loading tunnels was presented. In particular, a new discriminant indicator of asymmetric tunnels, named the asymmetric stress ratio, is introduced.

Based on the group's previous research, regardless of whether the surrounding rock is of grade III, IV_{Rock}, IV_{Soil} or V, the stress ratio of the arch wall is approximately 1.0, and the stress ratio of the arch foot has no obvious variation with increasing burial depth and decreasing surface slope angle. However, the stress ratio of the arch shoulder changes obviously. Due to space limitations, this article only introduces some of the main overviews of the stress ratio of the arch shoulder.

The asymmetric stress ratio is the ratio of the von Mises stress on symmetric left- and right-handed positions in the tunnel. Figure 2a shows points 1 and 2 that selected around the tunnel structure to analyze the asymmetric stress ratio. These points correspond to the left and right sides of the arch shoulder, respectively.

The stress ratio of the surrounding rock between points 1 and 2 of the arch shoulder is defined as Δ_1 :

$$\Delta_1 = \frac{\sigma_2}{\sigma_1} \quad (8)$$

where σ_1 and σ_2 are the von Mises stresses at key points 1 and 2, respectively.

3.2 Numerical Models of the Calculation

To give the quantitative criterion for discriminating asymmetric loading tunnels, the 269 kinds of models with different burial depths and different ground slopes under different surrounding rock grades were established, which consist of two types.

First, the 256 kinds of numerical models were established: the surrounding rock grades are III, IV_{Rock}, IV_{Soil} and V; the burial depths are 5 m, 10 m, 15 m, 20 m, 25 m, 30 m, 35 m and 40 m; and the surface slope angles are 5°, 10°, 15°, 20°, 25°, 30°, 35° and 40°. Second, the 13 kinds of numerical models based on the critical conditions of asymmetrical

loading tunnels listed in the Chinese Code for the Design of Railway Tunnels (TB 1003–2019) were established. Through the model calculations, the arch shoulder stresses of the surrounding rock are obtained, and the values of the asymmetric stress ratio are calculated.

4 Numerical Simulation Results and Discussion

4.1 Asymmetric Stress Ratio of Arch Shoulder

The 256 kinds of numerical models were established: The surrounding rock grades are III, IV_{Rock}, IV_{Soil} and V; the burial depths are 5 m, 10 m, 15 m, 20 m, 25 m, 30 m, 35 m and 40 m; and the surface slope angles are 5°, 10°, 15°, 20°, 25°, 30°, 35° and 40°. From the model calculations, the von Mises stresses of the surrounding rock at key points 1 and 2 corresponding to different numerical models were obtained. Then, based on Eq. (8), the asymmetric stress ratios were calculated.

Diagrams of the variation trends of the arch shoulder surrounding rock stress ratio for grades III, IV_{Rock}, IV_{Soil} and V are plotted with the changes in the burial depths and surface slope angles, as shown in Fig. 4.

As shown in Fig. 4, regardless of whether the surrounding rock is of grade III, IV_{Rock}, IV_{Soil} or V, the asymmetric stress ratio of the surrounding rock decreases and tends to stabilize with increasing burial depth and decreasing surface slope angle. When the surrounding rock is of grade III, the values of the stress ratio converge to approximately 1.64; when the surrounding rock is of grade IV_{Rock}, the values of the stress ratio converge to approximately 1.59; when the surrounding rock is of grade IV_{Soil}, the values of the stress ratio converge to approximately 1.54; and when the surrounding rock is of grade V, the values of the stress ratio converge to approximately 1.17. The asymmetric stress ratio decreases with decreasing surrounding rock grades.

Furthermore, from Fig. 4, two groups of behavior were clearly classified: Regardless of whether the surrounding rock is of grade III, IV_{Rock}, IV_{Soil} or V, slope angles between 5° and 20° show a gradual decrease, and slope angles between 25° and 40° show a rapid decrease when the burial depth is increased. Taking the burial depth of 5 m for example, when the slope angle is between 5° and 20° and the surrounding rock is of grade III, the values of stress ratio range from 1.17 to 2.74; when the surrounding rock is of grade IV_{Rock}, the values of stress ratio range from 1.15 to 2.53; when the surrounding rock is of grade IV_{Soil}, the values of stress ratio range from 1.13 to 2.30; when the surrounding rock is of grade V, the values of stress ratio range from 1.12 to 2.11; it can be seen from the above that the values of stress ratio decreases gradually, and the range of variation

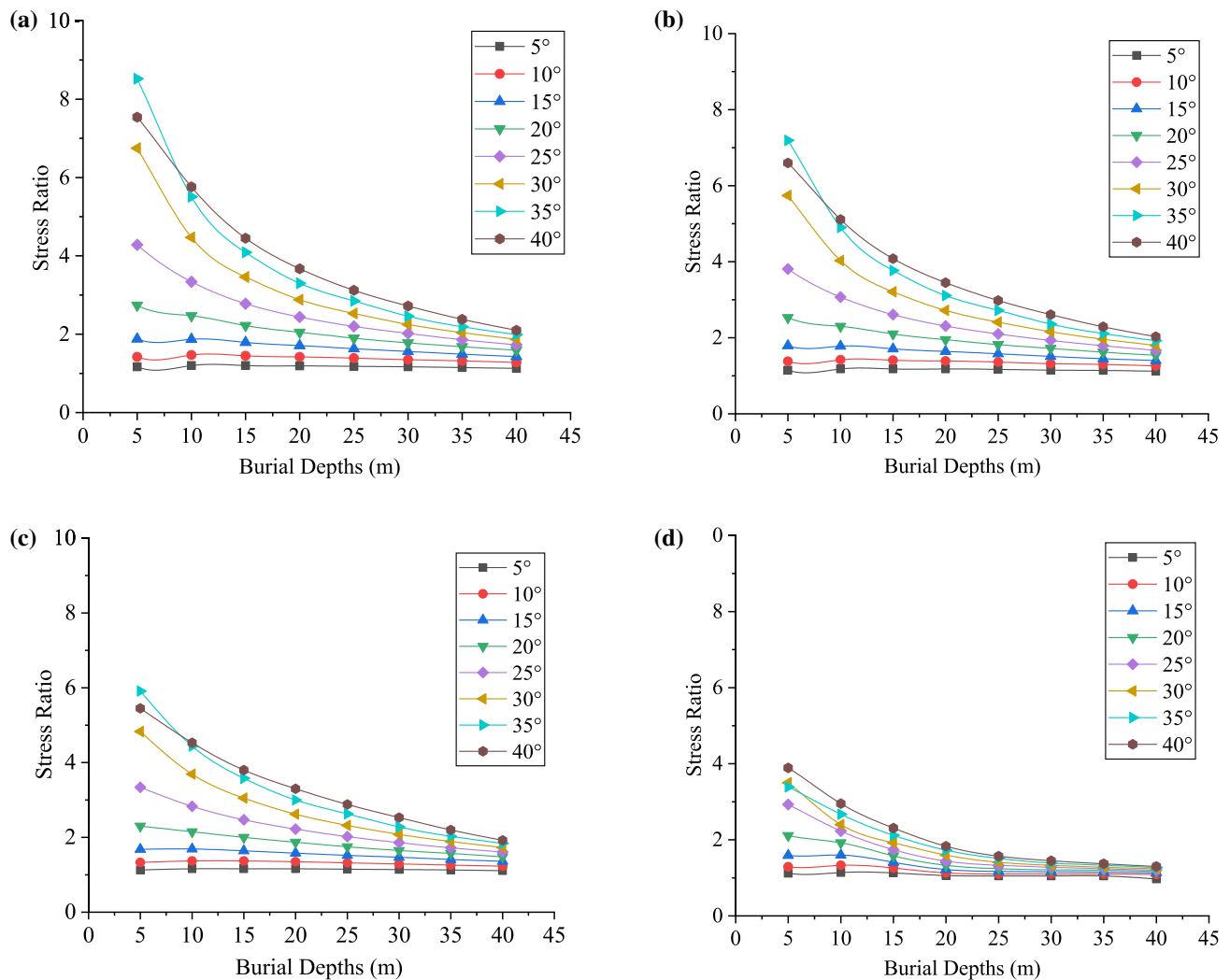


Fig. 4 Diagram of the variation trend of the asymmetric load stress ratio of surrounding rock: **a** grade III surrounding rock; **b** grade IV_{Rock} surrounding rock; **c** grade IV_{Soil} surrounding rock; **d** grade V surrounding rock

decreases gradually with the reduction in surrounding rock grades. When the slope angle is between 25° and 40° and the surrounding rock is of grade III, the values of stress ratio range from 4.28 to 8.52; when the surrounding rock is of grade IV_{Rock}, the values of stress ratio range from 3.81 to 7.19; when the surrounding rock is of grade IV_{Soil}, the values of stress ratio range from 3.34 to 5.91; when the surrounding rock is of grade V, the values of stress ratio range from 2.93 to 3.89; it can be seen from the above that the values of stress ratio decreases gradually, and the range of variation decreases gradually with the reduction in surrounding rock grades, but the range of stress ratio variation is significantly larger than that at 5°–20°. This phenomenon indicates that the sensitivity of the slope angle to the stress ratio increases after the slope angle exceeds 20°, and the effect of the asymmetric loads on the tunnel will be strengthened gradually.

Diagrams of the variation trends of the arch shoulder surrounding rock stress ratio for grades III, IV_{Rock}, IV_{Soil} and V are plotted in three-dimensional coordinates with the changes in the burial depths and surface slope angles, as shown in Fig. 5.

As seen from the diagram above, the stress ratio shows a good curve variation. Along with the decreasing burial depths and increasing surface slope angles, the stress ratio gradually reaches the maximum value; with the increasing burial depths and decreasing surface slope angles, the stress ratio gradually reaches the minimum value. When the surrounding rock is of grade III, the maximum stress ratio is 8.52; when the surrounding rock is of grade IV_{Rock}, the maximum stress ratio is 7.20; when the surrounding rock is of grade IV_{Soil}, the maximum stress ratio is 5.92; and when the surrounding rock is of grade V, the

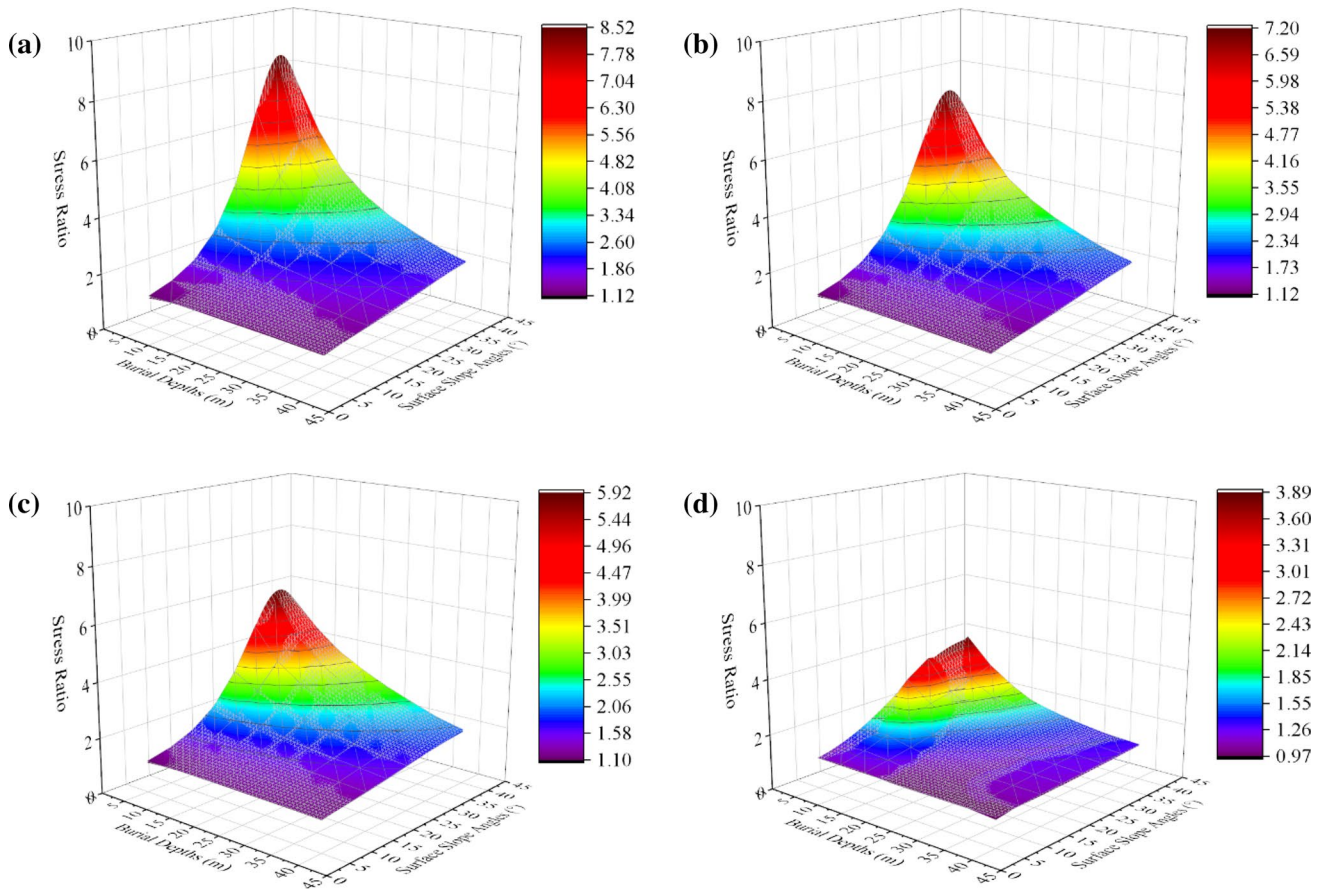


Fig. 5 Diagram of the variation trend of the surrounding rock stress ratio in three-dimensional coordinates: **a** grade III surrounding rock; **b** grade IV_{Rock} surrounding rock; **c** grade IV_{Soil} surrounding rock; **d** grade V surrounding rock

maximum stress ratio is 3.89. The values of the maximum stress ratio decrease with decreasing surrounding rock grades, and the values of the minimum stress ratio are all approximately 1.00, with little change.

Using a mathematical function, the three-dimensional surfaces were fitted in Fig. 5 to obtain the variation equation of the stress ratio with burial depths and surface slope angles under different surrounding rock grades. The equation of stress ratio is as Eq. (9).

$$\Delta_2 = \frac{A + Bh - C\alpha + D\alpha^2 - Eh\alpha}{1 + Fh - G\alpha + Hh^2 + I\alpha^2 - Jh\alpha} \quad (9)$$

where h is the burial depth (m), α is the surface slope angle ($^\circ$), Δ_2 is the stress ratio, and $A, B, C, D, E, F, G, H, I$ and J are parameters. The corresponding parameters are different at different grades of surrounding rock, as shown in Table 4.

When judging whether a tunnel is an asymmetric tunnel, it is only necessary to know the surrounding rock grade, burial depth and slope angle. The corresponding numerical model was established using finite element software, the surrounding rock stress of the arch shoulder was extracted, and

the stress ratio Δ_1 was calculated according to Eq. (8). The parameters in Eq. (9) were selected according to Table 4, and the corresponding burial depth and slope angle were entered to calculate the stress ratio Δ_2 .

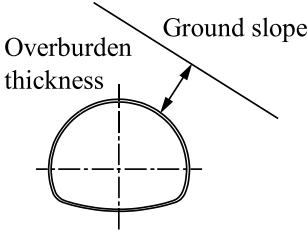
4.2 Asymmetric Critical Stress Ratio of Empirical Values

The data used to judge asymmetric tunnels in the Chinese Code are empirical data obtained from a large number of practical works. In general, determining whether a tunnel is subject to asymmetric loads is based on empirical values that are determined by the maximum burial depths and surface slope angles listed in the Chinese Code for the Design of Railway Tunnel (TB 1003–2019). When the vertical distance from the lateral arch shoulder of the tunnel to the surface is not more than the limit value listed in Table 5, the tunnel should be treated as being subjected to asymmetric loads. However, in real geological conditions, the maximum burial depths and surface slope angles of the tunnel are not necessarily completely consistent with the Chinese Code; in other words, the continuous discrimination of asymmetric

Table 4 Parameters of different grades of surrounding rock

	A	B	C	D	E	F	G	H	I	J
III	0.6759	0.0824	0.0118	0.0003	0.0008	0.0458	0.0596	0.0005	0.0009	0.0009
IV _{Rock}	0.7340	0.0727	0.0154	0.0003	0.0007	0.0428	0.0579	0.0004	0.0009	0.0008
IV _{Soil}	0.7910	0.0585	0.0196	0.0003	0.0006	0.0353	0.0559	0.0004	0.0008	0.0007
V	0.9339	0.0325	0.0220	0.0015	0.0001	0.0268	0.0508	-0.000009	0.0009	-0.0009

Table 5 Maximum burial depth above the lateral arch shoulder of a double-lined tunnel under asymmetric loads (m)

Ground slope	Surrounding rock grade				Sketch diagram
	III	IV _{Rock}	IV _{Soil}	V	
1:0.75	7	*	*	*	
1:1	7	*	*	*	
1:1.25	*	*	18	*	
1:1.5	7	11	16	30	
1:2	7	11	16	30	
1:2.5	*	*	13	20	

*Denotes a lack of statistical data, which can be obtained by analogous engineering values or empirical design values

tunnels is not realized. Therefore, Eq. (9) for the continuous identification of asymmetric tunnels was proposed, and a comparative analysis was performed with the corresponding empirical values of the Chinese Code.

Based on Table 5, numerical models of critical states for different surrounding rock grades are established to further verify the approach proposed above. The values of Von Mises stresses at key points in the surrounding rock are extracted, and the corresponding empirical values of asymmetric stress ratios are calculated according to Eq. (8). Furthermore, according to the critical states for different surrounding rock grades listed in Table 4, Table 5 and Eq. (9) proposed in this paper, the corresponding stress ratio is calculated.

The results are shown in Table 6, and the results were divided into three parts. In the first part, the surrounding rock grades are III and IV_{Rock}, and the ground slope is greater than or equal to 1:1.5; in the second part, the surrounding rock grades are III and IV_{Rock}, and the ground slope is 1:2; and in the third part, the surrounding rock grades are IV_{Soil} and V, and there is no restriction on the ground slope.

By comparing the stress ratios of the empirical value and equation value in Table 6, the following information is available. When the surrounding rock is of grade III, the empirical values are greater than the equation values. When the ground slope is greater than or equal to 1:1.5, there is a large difference between the empirical values and equation values. When the ground slope is 1:2, the empirical value

is basically the same as the equation value. When the surrounding rock is of grade IV_{Rock}, the empirical values are greater than the equation values. When the ground slope is greater than or equal to 1:1.5, there is a large difference between the empirical values and equation values. When the ground slope is 1:2, the difference between the empirical value and equation value is small. When the surrounding rock grades are IV_{Soil} and V, the equation values are in good agreement with the empirical values.

It can be seen from the above analysis that, in general, when the surrounding rock grades are III and IV_{Rock}, the empirical values are greater than the equation values, and the proposed approach in this paper is more conservative than the empirical method. When the surrounding rock grades are IV_{Soil} and V, the equation values are in good agreement with the empirical values. The proposed approach in this paper will provide significant insights for the continuous identification of asymmetrical loading tunnels, the design of support structures and the safety risk assessment of tunnels.

5 Summary and Conclusions

In this paper, based on numerical simulation, the asymmetric stress ratio for different slope angles and burial depths was analyzed in the presence of grades III, IV_{Rock}, IV_{Soil} and V surrounding rock, and a new approach to achieve the

Table 6 Surrounding rock stress ratio for different surrounding rock grades of the tunnel in the critical state

Ground slope	Surrounding rock grade							
	III		IV _{Rock}		IV _{Soil}		V	
	Empirical values	Equation values	Empirical values	Equation values	Empirical values	Equation values	Empirical values	Equation Values
1:0.75	4.93	3.07	*	*	*	*	*	*
1:1	5.78	5.33	*	*	*	*	*	*
1:1.25	*	*	*	*	3.45	3.58	*	*
1:1.5	6.85	5.98	4.42	3.49	3.34	3.11	1.38	1.34
1:2	4.38	4.37	3.22	2.96	2.58	2.59	1.29	1.28
1:2.5	*	*	*	*	2.19	2.24	1.37	1.42

continuous discrimination of asymmetric tunnels was proposed. Based on the achieved results, the following conclusions are drawn:

1. With decreasing surrounding rock grade, the asymmetric stress ratio tends to decrease. Regardless of whether the grade is III, IV_{Rock}, IV_{Soil} or V, the asymmetric stress ratios of the surrounding rock tend to converge and stabilize with increasing burial depths and decreasing dip angles, and the effect of the asymmetric loads on the tunnel will be weakened gradually.
2. The sensitivity of the slope angle to the stress ratio increased after the slope angle exceeded 20°, and the effect of the asymmetric loads on the tunnel will be strengthened gradually.
3. When the surrounding rock grades are III and IV_{Rock}, the values calculated using the proposed approach are lower than the empirical values, and the approach is more conservative than the empirical method. When the surrounding rock grades are IV_{Soil} and V, the values calculated using the proposed approach are in good agreement with the empirical values.
4. The asymmetric stress ratio of the surrounding rock arch shoulder can be used as an index to ascertain whether a tunnel is subjected to asymmetric loads. When the surrounding rock grades are III and IV_{Rock}, and the values of the stress ratio are greater than those calculated by Eq. (9), and when the surrounding rock grades are IV_{Soil} and V, the values of the stress ratio are greater than or approximately equal to those calculated by Eq. (9), and the tunnel can be considered to be in an asymmetrical loading state.

Acknowledgements This work is funded by the National Key Research and Development Program of China (No: 2018YFC1800900), the National Natural Science Foundation of China (Grant numbers: 41772253, 51974126, 51774136) and the Key Natural Science Foundation of Hebei Province (D2017508099). The authors also thank Jilin University (JLU) for the Program for JLU Science and Technology Innovative Research Team (JLUSTIRT-2019TD-35) and the Engineering Research Center of Geothermal Resources Development Technology and Equipment, Ministry of Education, China.

References

- Abdollahipour A, Rahmannedjad R (2012) Investigating the effects of lateral stress to vertical stress ratios and caverns shape on the cavern stability and sidewall displacements. *Arab J Geosci* 6:4811–4819
- Brown L, Hudyma M (2017) Identifying local stress increase using a relative apparent stress ratio for populations of mining-induced seismic events. *Can Geotech J* 54:128–137
- Cao XL, Guo WM, Zhou FX, Dai GL (2019) Stress analytical solution for shallow buried lined circular tunnel under the deformation of surrounding rock inner edge. *Geotech Geol Eng* 37:3771–3780
- Chen JX, Luo YB, Li Y, Zhao PY, Xu D, Wang QS (2020) The change of rock mass pressure of lianchengshan tunnel. *Environ Earth Sci* 79:192
- Do TN, Wu J (2020) Simulation of the inclined jointed rock mass behaviors in a mountain tunnel excavation using DDA. *Comput Geotech* 117:103249
- Hu ZN, Shen J, Wang YF, Guo TZ, Liu ZC, Gao XQ (2021) Cracking characteristics and mechanism of entrance section in asymmetrically-load tunnel with bedded rock mass: A case study of a highway tunnel in southwest China. *Eng Fail Anal* 122:105221
- Jiang XL, Wang FF, Yang H, Lian PY, Chen J, Niu JY, Sun GC (2018a) Dynamic response of shallow-buried tunnels under asymmetrical pressure distributions. *J Test Eval* 46:1574–1590
- Jiang X, Wang F, Yang H, Sun G, Niu J (2018b) Dynamic response of shallow-buried small spacing tunnel with asymmetrical pressure: shaking table testing and numerical simulation. *Geotech Geol Eng* 36:2037–2055
- Karatela E, Taheri A, Xu C, Stevenson G (2016) Study on effect of in situ stress ratio and discontinuities orientation on borehole

- stability in heavily fractured rocks using discrete element method. *J Petrol Sci Eng* 139:94–103
- Kong F, Lu D, Du X, Shen C (2019) Elastic analytical solution of shallow tunnel owing to twin tunnelling based on a unified displacement function. *Appl Math Model* 68:422–442
- Koopialipoor M, Ghaleini EN, Tootoonchi H, Armaghani DJ, Haghghi M, Hedayat A (2019) Developing a new intelligent technique to predict overbreak in tunnels using an artificial bee colony-based ANN. *Environ Earth Sci* 78:165
- Lei M, Peng L, Shi C, Xie Y, Tan L (2015a) Upper bound analytical solution for surrounding rock pressure of shallow unsymmetrical loading tunnels. *J Cent South Univ* 22:2339–2347
- Lei MF, Peng LM, Shi CH (2015b) Model test to investigate the failure mechanisms and lining stress characteristics of shallow buried tunnels under unsymmetrical loading. *Tunn Undergr Sp Technol* 46:64–75
- Lei M, Lin D, Yang W, Shi C, Peng L, Huang J (2016) Model test to investigate failure mechanism and loading characteristics of shallow-bias tunnels with small clear distance. *J Cent South Univ* 23:3312–3321
- Li W, Bai J, Li K, Zhang S (2020) Experimental analysis of deformation mechanics and stability of a shallow-buried large-span hard rock metro station. *Adv Civ Eng* 2020:4031306
- Lin L, Chen F, Huang Z (2019) An analytical solution for sectional estimation of stress and displacement fields around a shallow tunnel. *Appl Math Model* 69:181–200
- Liu XR, Chen HJ, Liu K, He CM (2017) Model test and stress distribution law of unsymmetrical loading tunnel in bedding rock mass. *Arab J Geosci* 10(7):1–11
- Lu W, Sun HB, Song SG, Ma WB, Wu YL, Guo XX (2021) Mechanical analysis of arch support and rock-arch interaction considering arch failure mechanism. *IJST T Civ Eng* 46(1):353–365
- Lv XB, Zhao QH, Han G (2017) Failure process of rock with single precast crack based on ratio of concentration stress to peak stress. *Rock Soil Mech* 38:87–95
- Ministry of Transport, People's Republic of China (2018) Specifications for design of highway tunnels (JTG 3370.1–2018). Beijing, China
- Nomikos PP, Yiouta-Mitra PV, Sofianos AI (2006) Stability of asymmetric roof wedge under nonsymmetric loading. *Rock Mech Rock Eng* 39:121–129
- Panji M, Koohsari H, Adampira M, Alielahi H, Asgari MJ (2016) Stability analysis of shallow tunnels subjected to eccentric loads by a boundary element method. *J Rock Mech Geotech* 8:480–488
- Papanikolaou VK, Kappos AJ (2014) Practical nonlinear analysis of unreinforced concrete tunnel linings. *Tunn Undergr Sp Technol* 40:127–140
- Qiu DH, Liu Y, Xue YG, Su MX, Zhao Y, Cui JH, Kong FM, Li ZQ (2021) Prediction of the surrounding rock deformation grade for a high-speed railway tunnel based on rough set theory and a cloud model. *IJST T Civ Eng* 45(1):303–314
- Railway Administration, People's Republic of China (2019) Code for design of railway tunnel (TB 1003–2019). Beijing, China
- Simanjuntak TDYF, Marencé M, Schleiss AJ, Mynett AE, Morris J, Chan A, Detwiler R, Hasenfus G, Huang H, Sanchez-Nagel M (2016) The interplay of in situ stress ratio and transverse isotropy in the rock mass on prestressed concrete-lined pressure tunnels. *Rock Mech Rock Eng* 49:4371–4392
- Wang ZR, Yuan SJ, Hu LX, Wang ZQ, He ZB (2007) Fundamentals of elasticity and plasticity. Harbin Institute of Technology press. Heilongjiang, China
- Wang SY, Sloan SW, Tang CA, Zhu WC (2012) Numerical simulation of the failure mechanism of circular tunnels in transversely isotropic rock masses. *Tunn Undergr Sp Technol* 32:231–244
- Xiao JZ, Dai FC, Wei YQ, Min H, Xu C, Tu XB, Wang ML (2014) Cracking mechanism of secondary lining for a shallow and asymmetrically loaded tunnel in loose deposits. *Tunn Undergr Sp Technol* 43:232–240
- Xiao JZ, Dai FC, Wei YQ, Xing YC, Cai H, Xu C (2016) Analysis of mechanical behavior in a pipe roof during excavation of a shallow bias tunnel in loose deposits. *Environ Earth Sci* 75(4):1–18
- Yang X, Zhang J, Jin Q, Ma J (2013) Analytical solution to rock pressure acting on three shallow tunnels subjected to unsymmetrical loads. *J Cent South Univ* 20:528–535
- Yang G, Zhang C, Cai Y, Min B (2019) Complex analysis of ground deformation and stress for a shallow circular tunnel with a cavern in the strata considering the gravity condition. *Ksce J Civ Eng* 23:4141–4153
- Yang C, Hu ZX, Huang D, Guo F (2020) Failure mechanism of primary support for a shallow and asymmetrically loaded tunnel portal and treatment measures. *J Perform Constr Fac* 34(1):04019105
- Yu QY, Song ZY, Du C, Dai ZX, Yin SX, Soltanian MR, Soltanian M, Liu W (2020) Analysis of asymmetric stress ratio in shallow buried tunnels. *Ksce J Civ Eng* 24:1924–1931
- Zhang ZQ, Li HY, Liu HY, Li GJ, Shi XQ (2014) Load transferring mechanism of pipe umbrella support in shallow-buried tunnels. *Tunn Undergr Sp Technol* 43:213–221
- Zhang ZG, Xu XY, Zhao QH (2016) Simple theoretical analysis of rock pressure for shallow unsymmetrical-loading tunnels considering horizontal earthquake action. *Rock Soil Mech* 37:16–24
- Zhang JW, Wan PP, Huang XM (2021) Three-dimensional limit equilibrium solution of minimum support pressure of shield tunnel face in sandy cobble stratum. *Arab J Sci Eng* 46:5061–5069
- Zhao YD, Shi Y, Yang JS (2021) Study of the concrete lining cracking affected by adjacent tunnel and oblique bedded rock mass. *IJST T Civ Eng* 45(4):2853–2860
- Zou J, Wei A, Yang T (2018) Elasto-plastic solution for shallow tunnel in semi-infinite space. *Appl Math Model* 64:669–687
- Zuo CQ, Chen JP, Liu H (2011) Load calculation method of tunnels with shallow buried depth and unsymmetrical pressure in regions of weak fissured surrounding rock. *Adv Mater Res* 243:3364–3369
- Zuo QJ, Wu L, Lu ZL, Tan YZ, Yuan Q (2015) Instability analysis of soft surrounding rock in shallow tunnel portal under unsymmetrical pressure by catastrophe theory. *Rock Soil Mech* 36:424–430

Springer Nature or its licensor holds exclusive rights to this article under a publishing agreement with the author(s) or other rightsholder(s); author self-archiving of the accepted manuscript version of this article is solely governed by the terms of such publishing agreement and applicable law.